

Did the Universe Reheat After Recombination?

J. Colin Hill^{1,2,*} and Boris Bolliet^{3,1,†}

¹*Department of Physics, Columbia University, New York, NY 10027, USA*

²*Center for Computational Astrophysics, Flatiron Institute, New York, NY 10010, USA*

³*DAMTP, Centre for Mathematical Sciences, Wilberforce Road, Cambridge CB3 0WA, UK*

A key assumption of the standard cosmological model is that the temperature of the cosmic microwave background (CMB) radiation scales with cosmological redshift z as $T_{\text{CMB}}(z) \propto (1+z)$ at all times after recombination at $z_* \simeq 1090$. However, this assumption has only been precisely tested at $z \lesssim 3$. Here, we consider cosmological models with post-recombination reheating (PRR), in which the CMB monopole temperature abruptly increases due to energy injection after last scattering. Such a scenario can potentially resolve tensions between inferences of the current cosmic expansion rate (the Hubble constant, H_0). We consider an explicit model in which a metastable sub-component of dark matter (DM) decays to Standard Model photons, whose spectral energy distribution is assumed to be close to that of the CMB blackbody. A fit to *Planck* CMB anisotropy, *COBE/FIRAS* CMB monopole, and SH0ES distance-ladder measurements yields $H_0 = 71.2 \pm 1.1$ km/s/Mpc, matter fluctuation amplitude $S_8 = 0.774 \pm 0.018$, and CMB temperature increase $\delta T_{\text{CMB}} = 0.109^{+0.033}_{-0.044}$ K, which is sourced by DM decay at $z \gtrsim 10$. However, matter density constraints from baryon acoustic oscillation and supernovae data highly constrain this scenario, with a joint fit to all datasets yielding $H_0 = 68.69 \pm 0.35$ km/s/Mpc, $S_8 = 0.8035 \pm 0.0081$, and $\delta T_{\text{CMB}} < 0.0342$ K (95% CL upper limit). These bounds can be weakened if additional dark relativistic species are present in the early universe, yielding higher H_0 . We conclude that current data disfavor models with significant PRR solely through its impact on background and linear-theory observables, completely independent of CMB spectral distortion constraints. However, a small amount of such energy injection could play a role in restoring cosmological concordance.

PACS numbers: 98.80.-k, 98.70.Vc, 98.80.Es, 98.80.Cq

Introduction—Recent observations suggest that the current standard model of cosmology, Λ cold dark matter (Λ CDM), may no longer provide an acceptable description of our Universe. While Λ CDM provides a good fit to data from cosmic microwave background (CMB) experiments [1–4], the predictions of the best-fit model to CMB data are in moderate disagreement with some direct probes of the cosmic expansion rate (the Hubble constant, H_0) [5–8] and the low-redshift matter clustering amplitude (parameterized by $S_8 \equiv \sigma_8 \sqrt{\Omega_m/0.3}$, where σ_8 is the root-mean-square linear-theory matter fluctuation amplitude at redshift $z = 0$ and Ω_m is the matter density today in units of the critical density) [9–14]. Indeed, the discrepancy in H_0 is not unique to CMB data, as large-scale structure (LSS) data analyses yield similar results [15–17], lower than direct measurements. However, the observational situation is not fully clear, as some direct H_0 measurements are not in tension with the CMB and LSS constraints [18–21], and some probes of S_8 are not in tension with the CMB [16, 22]. For a comprehensive account of recent measurements, see, e.g., Refs. [23, 24].

Nevertheless, the growing number of independent probes yielding similarly anomalous results suggests that the H_0 and S_8 tensions may indeed reflect a shortcoming of Λ CDM, and thus a sign of new physics. In recent years, many scenarios have been explored, with varying degrees of success [23–26]. Here we test an underlying assumption of the cosmological model that has evaded at-

tention thus far, motivated by the approach of Ref. [27], who showed that CMB data could accommodate a high H_0 value by lowering the monopole CMB temperature, $T_{\text{CMB},0} \equiv T_{\text{CMB}}(z = 0)$, from its standard Λ CDM value (2.7255 K [28]) to $T_{\text{CMB},0} = 2.56 \pm 0.05$ K (68% CL). This exploits a degeneracy $H_0 \propto T_{\text{CMB},0}^{-1.2}$ in Λ CDM [see 27, for details], hinting that the H_0 tension can be recast as a tension between CMB anisotropy data combined with local H_0 probes and the *COBE/FIRAS* measurement of $T_{\text{CMB},0}$ [28, 29]. Unfortunately, the *FIRAS* error bar on $T_{\text{CMB},0}$ is so small (≈ 1 mK) [28] that no plausible systematic error could bias $T_{\text{CMB},0}$ by a sufficient amount to actually resolve the H_0 tension in this minimal, theoretically appealing scenario (see also Refs. [30, 31] for related discussion).

Motivated by this observation, here we consider a cosmology with lower-than-standard $T_{\text{CMB}}(z)$ at $z > z_*$, where $z_* \simeq 1090$ is the redshift of recombination. The *FIRAS* measurement of $T_{\text{CMB},0}$ is accommodated via a brief epoch of post-recombination “reheating” (PRR) during which the usual scaling $T_{\text{CMB}}(z) \propto (1+z)$ is violated. Due to the transient nature of the PRR epoch, this scenario differs from models in which $T_{\text{CMB}}(z) \propto (1+z)^\alpha$ with $\alpha \neq 1$, which are tightly constrained by observations at $z \lesssim 3$ (e.g., [32–35]). For simplicity, we assume that the injected energy is thermal, but note that PRR scenarios with a wide range of injected photon energies are not ruled out by *FIRAS* or other data [36]. One might expect that a PRR model would decrease the

sound horizon at last scattering via earlier recombination due to the lower $T_{\text{CMB}}(z \gtrsim z_*)$, similar in spirit to other modified-recombination proposals (e.g., [37–40]). However, the sound horizon is actually *not* decreased relative to ΛCDM , because of the lower radiation density at early times. Instead, the PRR scenario yields a higher H_0 via an interplay of pre- and post-recombination quantities (see Ref. [41], hereafter BH23, for details).

To implement the scenario concretely, we consider a model with a sub-component of decaying (or de-exciting) cold dark matter (DCDM) that produces photons at some redshift z_X , with $z_X < z_*$ (“DCDM γ ” hereafter). The decay is assumed to take place prior to the era in which direct constraints on $T_{\text{CMB}}(z)$ exist (i.e., $z_X \gtrsim 3$).¹ The decay products are assumed to be thermal, such that no significant CMB spectral distortion is generated; we discuss this assumption further below and demonstrate in BH23 that viable parameter space exists. Regardless, the constraints that we obtain effectively follow directly from the agreement of the *FIRAS* measurement of $T_{\text{CMB},0}$ [28] and the indirect inference of $T_{\text{CMB},0}$ from (non-*FIRAS*) cosmological datasets [27], independent of any spectral distortion signatures. The relevant mass range of the DCDM is sufficiently low ($\lesssim \text{eV}$) in such models that the metastable component could yield an additional contribution to N_{eff} (the effective number of relativistic species) at z_* ; we thus consider a model extension in which N_{eff} is also a free parameter.

Theory— The evolution of the background (average) DCDM energy density, ρ_{DCDM} , and the photon energy density, ρ_γ , in our model are, respectively:

$$\rho'_{\text{DCDM}} = -3aH\rho_{\text{DCDM}} - a\Gamma\rho_{\text{DCDM}} \quad (1)$$

$$\rho'_\gamma = -4aH\rho_\gamma + a\Gamma\rho_{\text{DCDM}}, \quad (2)$$

where $a = (1+z)^{-1}$ is the cosmic scale factor, primes denote derivatives with respect to conformal time τ (defined by $d\tau = dt/a$ where t is the cosmic time), $H(a) = (da/dt)/a$ is the Hubble parameter defined with respect to cosmic time (thus $aH = a'/a$), and Γ is the DCDM decay rate defined with respect to cosmic time. These equations follow directly from covariant conservation of the stress-energy tensor for the combined DCDM+ γ system, and are analogous to those in models with DCDM decaying into dark radiation (DCDM-DR) (e.g., [43, 44]). Throughout, we assume a spatially flat universe.

The linear perturbation evolution equations for our model are similar to those of the DCDM-DR model, but some important differences arise due to the decay of the DCDM into Standard Model photons in our scenario.

¹ Note that in, e.g., decaying axion models the decay rate can be significantly enhanced due to stimulated emission associated with the temperature of an ambient photon bath, which could play a role here [42].

Parameter	Prior
$\hat{\omega}_b$	[0.005, 0.1]
$\hat{\omega}_c$	[0.001, 0.99]
$\ln(10^{10} \hat{A}_s)$	[1.61, 3.91]
n_s	[0.8, 1.2]
$100\theta_s$	[0.5, 10]
τ_{reio}	[0.01, 0.8]
$T_{\text{CMB},\text{ini}}/\text{K}$	[2.3, 3.5]
$\log_{10}(\hat{\omega}_{\text{DCDM},\text{ini}})$	[-5, 0]
$\log_{10}(\Gamma/(\text{km/s/Mpc}))$	[2, 6]
N_{eff}	[0.01, 10]

TABLE I: DCDM γ model parameters and uniform prior ranges used in MCMC analyses; we list N_{eff} separately as it is an extension of the base model.

We provide the perturbation equations of motion in the Supplemental Material.

We now briefly describe the parametrization of our model, as implemented in our modified version of the Einstein-Boltzmann solver **CLASS** [45]. We first define the temperature that the CMB photons would have at $z = 0$ (today) *if* no DCDM existed, $T_{\text{CMB},\text{ini}}$ (the subscript indicates that this quantity characterizes the photons at early times). We then define $\delta T_{\text{CMB}} \equiv T_{\text{CMB},0} - T_{\text{CMB},\text{ini}}$, the amount by which the CMB temperature today has been increased due to the DCDM, as compared to a no-DCDM universe. Note that *FIRAS* data require $T_{\text{CMB},0} \approx 2.7255 \text{ K}$. We then define the would-be density fraction in DCDM at $z = 0$ if there had been no decay, $\Omega_{\text{DCDM},\text{ini}}$ (or $\omega_{\text{DCDM},\text{ini}} \equiv \Omega_{\text{DCDM},\text{ini}} h^2$),² which sets the initial DCDM density in the early universe: $\rho_{\text{DCDM}}(z_{\text{ini}}) = \Omega_{\text{DCDM},\text{ini}} \rho_{\text{crit},0} (1 + z_{\text{ini}})^3$, with $1 + z_{\text{ini}} = 10^{14}$ (**CLASS** default). The initial density of decay photons also has an analytic form (proportional to Γ) [43], although it is very close to zero for the models of interest. We define N_{eff} with respect to $T_{\text{CMB},\text{ini}}$, as this is the relevant radiation energy density at high redshift: $\rho_{\text{ur},0} = N_{\text{eff}}(7/8)(4/11)^{4/3}(4\sigma_B T_{\text{CMB},\text{ini}}^4)$, where $\rho_{\text{ur},0}$ is the energy density in ultra-relativistic (light) species today and σ_B is the Stefan-Boltzmann constant.³

Linear-theory CMB and LSS power spectra are nearly invariant under a certain rescaling of the cosmological parameters [27, 46], which motivates a reformulation of the fundamental cosmological parameter set in models with $T_{\text{CMB},0}$ allowed to vary. Here we adapt the param-

² As usual, $\Omega_i \equiv (\rho_{i,0}/\rho_{\text{crit},0})$ is the energy density fraction in component i at $z = 0$ (today), where $\rho_{\text{crit},0} = 3H_0^2/(8\pi G)$ is the critical density today (G is Newton’s constant), and $\omega_i \equiv \Omega_i h^2$, with $h \equiv H_0/(100 \text{ km/s/Mpc})$.

³ In practice, we sample in terms of the **CLASS** parameter N_{ur} and treat N_{eff} as derived.

eterization from Ref. [27] to our scenario:

$$\hat{\omega}_b \equiv \omega_b \left(\frac{T_{\text{CMB,ini}}}{T_{\text{FIRAS}}} \right)^{-3} \quad (3)$$

$$\hat{\omega}_c \equiv \omega_c \left(\frac{T_{\text{CMB,ini}}}{T_{\text{FIRAS}}} \right)^{-3} \quad (4)$$

$$\hat{\omega}_{\text{DCDM,ini}} \equiv \omega_{\text{DCDM,ini}} \left(\frac{T_{\text{CMB,ini}}}{T_{\text{FIRAS}}} \right)^{-3} \quad (5)$$

$$\hat{A}_s \equiv A_s \left(\frac{T_{\text{CMB,ini}}}{T_{\text{FIRAS}}} \right)^{n_s-1}. \quad (6)$$

with $T_{\text{FIRAS}} = 2.7255$ K. Sampling the posterior in these parameters is more efficient [27]. The complete set of free parameters in our model and the priors used in our Markov Chain Monte Carlo (MCMC) analyses are given in Table I. We adopt uniform priors on $\log_{10}(\hat{\omega}_{\text{DCDM,ini}})$, as this quantity is expected to be small, and on $\log_{10}(\Gamma)$, to explore a wide range of decay redshifts. We have validated our implementation against that of Ref. [27] for models with $T_{\text{CMB},0} \neq 2.7255$ K (but with $T_{\text{CMB}}(z) \propto (1+z)$), to ensure that subtleties related to Big Bang nucleosynthesis (BBN) and CMB modeling (see [27]) are treated properly.

Following *Planck* [31], we fix the sum of the neutrino masses to $\sum m_\nu = 0.06$ eV, with one massive eigenstate and two massless eigenstates. The primordial helium fraction is computed via BBN. Nonlinear effects in the matter power spectrum are calculated via *Halofit* [47, 48], although the observables we consider are dominated by linear modes.

Phenomenology— In the DCDM γ model, a natural expectation is that the redshift of recombination, z_* , can be increased by lowering $T_{\text{CMB,ini}}$, thus yielding a smaller sound horizon, r_s^* . However, the decrease in the radiation density due to the lower $T_{\text{CMB,ini}}$, and hence the decrease in $H(z)$ in the early universe, actually leads to an *increase* in r_s^* . To keep $\theta_s \equiv r_s^*/D_A^*$ fixed, the angular diameter distance to recombination, $D_A^* = \int_0^{z_*} c dz/H(z)$, must also increase. However, due to the increase in z_* , the integral appearing in D_A^* actually increases by too much, and one must *increase* H_0 to compensate for this and leave θ_s unchanged. In addition, to keep k_{eq} (the scale of matter-radiation equality) fixed, the matter density must decrease, which decreases S_8 (the small amount of dark matter that decays also helps in this regard). When fit to CMB data, the PRR scenario thus naturally moves both H_0 and S_8 toward values that relax tensions with direct probes;⁴ an increase $\delta T_{\text{CMB}} \approx 100$ mK in the post-

recombination epoch would suffice to resolve the discrepancies.

Generically, achieving this phenomenology requires the DCDM to decay after recombination. Due to observational constraints requiring $T_{\text{CMB}}(z) \propto (1+z)$ at $z \lesssim 3$ (e.g., [32–35]), we thus expect the DCDM to decay during matter domination.⁵ During this epoch, the DCDM decay redshift, z_X , is well-approximated by [36] $z_X \approx 0.812 (\Gamma/H_0)^{2/3} (0.3/\Omega_m)^{1/3}$; e.g., $\Gamma = 10^4$ km/s/Mpc yields $z_X \approx 22$. Our prior range for Γ (c.f. Table I) thus corresponds to $1 \lesssim z_X \lesssim 500$. A crucial feature of decay during matter domination is that even a small fraction of DCDM can inject enough energy to change T_{CMB} significantly, since $\rho_c(z) \gg \rho_\gamma(z)$ during this epoch. For example, at $z_X = 22$, $\rho_c \approx 210 \rho_\gamma$, and thus increasing ρ_γ by 4% at this epoch (i.e., increasing $T_{\text{CMB}}(z=22)$ by 1%) requires only $\simeq 0.02\%$ of the CDM to decay. Thus, our prior range on the DCDM density extends to very small values (c.f. Table I), motivating the use of a uniform logarithmic prior.

A crucial assumption underlying our model is that the photon distribution function maintains its blackbody form to guarantee consistency with *FIRAS* data, which severely constrain CMB monopole spectral distortions [29, 36, 50]. We assume that the injected energy is fully thermal and simply increases the monopole CMB temperature. If photons are injected near the peak of the CMB monopole (≈ 160 GHz today), *FIRAS* constrains the relative amount of decaying DM, $f_{\text{DCDM}} \equiv \omega_{\text{DCDM,ini}}/\omega_{c,\text{ini}}$, to $f_{\text{DCDM}} \lesssim 10^{-4}$ [36]. Nonetheless, if the injection happens at frequencies a factor of a few lower than or a factor of 100 higher than the peak, f_{DCDM} is not constrained because for such photons the universe is transparent and no spectral distortion is generated in the *FIRAS* frequency range (see [36] and BH23 for further details). However, one would need to track the full set of spatial-spectral equations in such models [51–53], as the radiation would no longer be blackbody. Here we adopt the simpler approach of assuming that the injected radiation is thermal; at the background level, particularly for H_0 , this assumption makes no difference. Although it is challenging to construct models that fully thermalize extra radiation in the post-recombination universe [54], injecting photons outside the range constrained by *FIRAS* is straightforward. Here we assume that linear perturbation theory in such models is well-approximated by our approach, given that the injected energy and f_{DCDM} are quite small. This assumption will be weakly violated

⁴ The background physics underlying the increase in H_0 is identical to that in Λ CDM with varying $T_{\text{CMB},0}$ [27]; the changes in $H(z)$ due to PRR are very small, and its primary role is to match *FIRAS*. Furthermore, the novel terms in the perturbation

evolution equations in DCDM γ play an almost negligible role in the CMB fit (see BH23).

⁵ A constraint on T_{CMB} at $z = 6.34$ was recently reported [49]; however, the error bar is sufficiently large to encompass the small temperature change in the model proposed here, and we are primarily focused on changes to T_{CMB} at higher redshifts.

in a full particle physics model, but corrections to the above equations will necessarily be small if the model is to satisfy the *FIRAS* constraints.

BBN abundance constraints are another potential challenge. However, we demonstrate in the Supplemental Material that the $\Lambda\text{CDM}\gamma$ and $\Lambda\text{CDM}\gamma+N_{\text{eff}}$ models both fit BBN data well.

Data— We constrain the $\Lambda\text{CDM}\gamma(+N_{\text{eff}})$ parameters using the following datasets:

- *FIRAS* $T_{\text{CMB},0}$: Fixsen (2009) [28] measurement of $T_{\text{CMB},0} = 2.72548 \pm 0.00057$ K;
- *CMB* $TT+TE+EE$: *Planck* PR3 (2018) primary CMB TT, TE, and EE power spectra [2, 31, 55];
- *CMB* *Lensing* $\phi\phi$: *Planck* PR3 reconstructed CMB lensing potential power spectrum [22];
- *BAO*: Baryon acoustic oscillation (BAO) distances from SDSS [56, 57] and 6dF [58];
- *SN Ia*: Pantheon Type Ia supernova (SNIa) distances [59];
- *RSD*: Redshift-space distortion (RSD) constraints on $f\sigma_8(z)$ from SDSS [57, 60] (we include the BAO-RSD covariance);
- *DES-Y3*: DES-Y3 [9] measurement of $S_8 = 0.776 \pm 0.017$ (we verify in BH23 that the full DES “ $3\times 2\text{pt}$ ” likelihood is well-approximated by this prior on S_8 using the same approach as in [61]);
- *SH0ES*: Direct constraint on H_0 from Cepheid-calibrated SNIa ($H_0 = 73.2 \pm 1.3$ km/s/Mpc) [6];
- *Combined* H_0 : Inverse-variance-weighted combination of direct constraints on H_0 from three independent probes: SH0ES, TRGB-calibrated surface brightness fluctuations translated into the 2M++ frame ($H_0 = 73.6 \pm 3.6$ km/s/Mpc) [8], and megamaser distances with peculiar velocity corrections in the 2M++ frame ($H_0 = 70.1 \pm 2.9$ km/s/Mpc) [20], yielding $H_0 = 72.8 \pm 1.1$ km/s/Mpc.⁶

We sample the parameter posteriors using the MCMC code *Cobaya* [62] coupled to our modified *CLASS*. We consider our MCMC chains converged when the Gelman-Rubin [63] criterion $R - 1 < 0.03$.

Results— The main results of our analysis are presented in Fig. 1. In the Supplemental Material, we include full numerical constraints (Table III) and results for $\Lambda\text{CDM}\gamma+N_{\text{eff}}$ (Table IV and Fig. 2).⁷ For $\Lambda\text{CDM}\gamma$, primary CMB data alone show no preference for the model over ΛCDM .⁸ However, the inclusion of SH0ES H_0 data leads to a mild preference for non-zero DCDM: $\log_{10}(\hat{\omega}_{\text{DCDM},\text{ini}}) = -3.77^{+0.66}_{-1.1}$, and an accordingly higher $H_0 = 71.2 \pm 1.1$ km/s/Mpc and lower $S_8 = 0.774 \pm 0.018$ with $\delta T_{\text{CMB}} = 0.109^{+0.033}_{-0.044}$ K. The fit to *Planck* CMB data is slightly degraded, with $\Delta\chi^2_{\text{Planck}} = 6.7$ compared to the best-fit ΛCDM model to *Planck* alone. Removing SH0ES but including the full suite of non- H_0 datasets (“walking barefoot” [61]), the preference for DCDM weakens but is somewhat stronger than for primary CMB data alone, due to the influence of the DES-Y3 S_8 constraint. Using all datasets, including all three independent H_0 probes, we find $H_0 = 68.69 \pm 0.35$ km/s/Mpc, $S_8 = 0.8035 \pm 0.0081$, and $\delta T_{\text{CMB}} < 0.0342$ K (95% CL upper limit). Interestingly, the fit to *Planck* is not degraded compared to that of ΛCDM , with $\Delta\chi^2_{\text{Planck}} = 0.3$, even though H_0 increases by 2.5σ from its ΛCDM value (67.36 ± 0.54 km/s/Mpc) [31].

Although the DCDM component is not strongly detected, all dataset combinations exclude low values of Γ (i.e., low z_X). In the *Planck*+*FIRAS*+SH0ES analysis, the best-fit $z_X \simeq 40$; in the joint analysis of all datasets, the best-fit $z_X \simeq 190$ (and $z_X \gtrsim 10$ at 95% CL). The (mildly) preferred decay redshifts are thus prior to reionization, where no direct observational constraints exist.

A key takeaway is that a small amount of DCDM can significantly affect the radiation energy density during this epoch. In the *Planck*+*FIRAS*+SH0ES analysis, the best-fit $f_{\text{DCDM}} = 0.332\%$, yielding $\delta T_{\text{CMB}} = 0.138$ K; in the joint analysis of all datasets, the best-fit $f_{\text{DCDM}} = 0.153\%$, yielding $\delta T_{\text{CMB}} = 0.0169$ K. Notably, our upper bounds on f_{DCDM} are an order of magnitude below those on the energy density of massive neutrinos, $\omega_\nu/\omega_c \lesssim 1.1\%$ [31]; thus, any effects on early structure formation due to the potentially large thermal velocities of the DCDM component are negligible.

The primary obstacle to further increasing H_0 in the global fit to $\Lambda\text{CDM}\gamma$ comes from the independent constraint on Ω_m from the BAO and SNIa data, which do not allow Ω_m to take the low value obtained in the fit to *Planck*+*FIRAS*+SH0ES. This low value of Ω_m is needed to maintain k_{eq} in the fit to *Planck*, due to the decreased

⁶ Our results would be nearly unchanged if we instead used the most recent SH0ES measurement on its own, $H_0 = 73.04 \pm 1.04$ km/s/Mpc [7]. However, the mild preference that we find for the $\Lambda\text{CDM}\gamma$ model would be weakened if we instead used $H_0 = 69.8 \pm 0.6$ (stat.) ± 1.6 (syst.) km/s/Mpc from TRGB-calibrated SNIa [19].

⁷ We also explore an extension with varying curvature density Ω_k , but find that the $\Lambda\text{CDM}\gamma$ constraints are generally within 1σ of those in the $\Omega_k = 0$ case.

⁸ Marginalization effects (e.g., [64]) associated with the prior volume of Γ in the $\omega_{\text{DCDM}} \rightarrow 0$ limit could mildly bias constraints toward ΛCDM in this analysis.

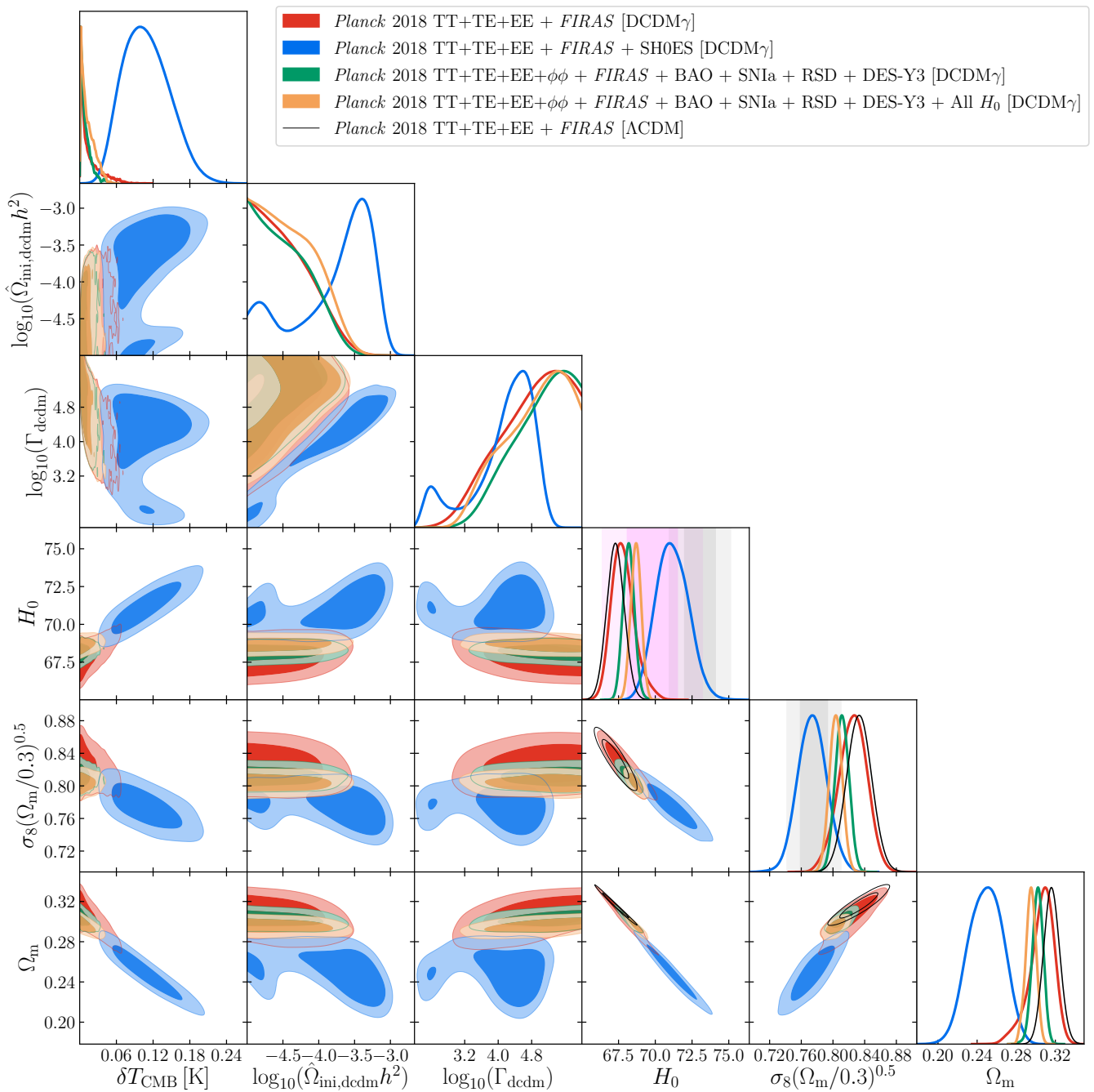


FIG. 1: Marginalized posteriors for the DCDM γ parameters and select other parameters in fits to various datasets, as labeled, with H_0 and Γ in units of km/s/Mpc. For comparison, Λ CDM constraints for *Planck* CMB and *FIRAS* data are shown in thin black lines. The vertical grey and magenta bands in the H_0 panel show the latest SH0ES [7] and TRGB [19] measurements, respectively. The vertical grey band in the S_8 panel shows the DES-Y3 constraint [9].

radiation density at early times. A simple remedy to this problem is to introduce additional relativistic energy density in the early universe via $N_{\text{eff}} > 3.044$. Results of this analysis are reported in the Supplemental Material.

Outlook— In this work, we have investigated the extent to which cosmological data permit PRR, even if the injected photons preserve the CMB blackbody form. In

the DCDM γ model, we find tight limits, with $\delta T_{\text{CMB}} < 0.0342$ K (95% CL, all datasets). These constraints are fully independent from CMB spectral distortion probes, and similarly tight bounds should hold for other specific PRR models. Such a reheating episode could play a role in resolving current tensions between inferences of H_0 and S_8 , although constraints on Ω_m obstruct a complete

resolution without further modifications.

The PRR impact on H_0 differs from the modified recombination scenario of Ref. [37], who suggest a modification to the CMB spectrum deep in the Wien tail, where *FIRAS* constraints are absent ($\gtrsim 1.5$ THz); such a model does not change $\rho_\gamma(z)$ significantly, instead only removing a small fraction of the high-energy photons to change the timing of recombination. Our scenario also differs from modified-recombination models that increase H_0 via a decrease in r_s^* , such as via primordial magnetic fields (e.g., [39, 40]) or an increase in the electron mass (e.g., [38, 65, 66]). In contrast, r_s^* (slightly) increases in the PRR scenario, and H_0 is increased due to the interplay with D_A^* discussed earlier.

Tighter PRR constraints can be obtained using CMB data from the Atacama Cosmology Telescope [3, 67] and galaxy clustering data from the Baryon Oscillation Spectroscopic Survey (BOSS) [17], amongst other probes [68]. Moreover, the difference in the spectral energy distribution of the CMB anisotropies in PRR scenarios compared to that of the monopole at $z = 0$ leads to spatial-spectral distortions, which can be constrained via the formalism of Refs. [51–53]; this approach is formally necessary for models in which the DCDM produces photons in a line outside the *FIRAS* frequency range (thus increasing ρ_γ , but in a non-thermal sub-component).

Many models have been constructed in which dark states decay through various channels that eventually cascade to photons (e.g., [69–75]), or in which metastable vacuum decay produces additional photons [76–79]. Ref. [80] considered a scenario similar to ours, but with decays prior to recombination rather than afterward, finding tight bounds solely from background cosmological signatures. Models with heavier DM decaying to higher-energy photons (\gtrsim keV) have been constrained via their impact on the ionization and thermal history of the universe, searches for direct signatures in X-ray and γ -ray data, and other probes (e.g., [31, 69, 81–87]); we have considered a scenario in which such bounds are negligible due to the low energy of the decay photons.

Small modifications of the DCDM γ scenario considered here may be necessary to evade bounds from stellar cooling and supernovae (e.g., [88–90]). This can be achieved by replacing the particle decay process with radiation arising from the decay of an excited state in the dark sector to its ground state (e.g., [91–94]). In this model, the DM possesses a dipole moment and couples to the Standard Model through a kinetically mixed massive dark photon, which allows for transitions between the ground and excited DM states. For an energy splitting $\simeq 0.1$ eV between these states, and theoretically reasonable transition dipole moments, the model yields lifetimes $\simeq 1 - 10$ Myr (see Eq. 2.2 of [93]), which is exactly the regime of interest for the DCDM γ scenario. If the massive dark photon is heavier than an MeV, it is not produced in stars or supernovae, and bounds on

interactions today are irrelevant since essentially all of the energy density will have decayed away by the present time. The primary change to the model considered here is the treatment of the DCDM density, but this is already constrained to be sufficiently small that we expect our implementation to yield similar results to this approach, which we leave to future work.

Our results indicate that, independent of spectral distortion constraints, cosmological data allow only small changes to the photon energy density between recombination and the present era. Fundamentally, this arises from the agreement between the *FIRAS* direct measurement of $T_{\text{CMB},0}$ [28] and the indirect inference from CMB, BAO, and other data [27]. Future high-precision CMB spectrometers can further constrain PRR models [95–99].

Acknowledgments. We are grateful to Ameya Chavda, Fiona McCarthy, Adam Riess, and Ken van Tilburg for useful exchanges, and especially to Mikhail Ivanov for helpful comments and providing code from Ref. [27] for validation. JCH acknowledges support from NSF grant AST-2108536, NASA grants 21-ATP21-0129 and 22-ADAP22-0145, DOE grant DE-SC00233966, the Sloan Foundation, and the Simons Foundation. We thank the Scientific Computing Core staff at the Flatiron Institute for computational support. The Flatiron Institute is supported by the Simons Foundation. BB acknowledges support from the European Research Council (ERC) under the European Union’s Horizon 2020 research and innovation programme (Grant agreement No. 851274). We acknowledge use of the `matplotlib` [100], `numpy` [101], `GetDist` [102],⁹ and `Cobaya` [62]¹⁰ packages, use of the Boltzmann code `CLASS` [45],¹¹ and use of the BBN code `PRIMAT` [103, 104].¹²

⁹ <https://github.com/cmbant/getdist>

¹⁰ <https://github.com/CobayaSampler/cobaya>

¹¹ <http://class-code.net/>

¹² <http://www2.iap.fr/users/pitrou/primat.htm>

Supplemental Material

Linear Perturbation Evolution Equations

For component i , defining the density perturbation $\delta_i \equiv \rho_i/\bar{\rho}_i - 1$ and the velocity divergence $\theta_i \equiv ik^j v_j$ where k^j is the Fourier-space wavevector (we follow the definitions and notation of [105]), the evolution of the DCDM and photon perturbations are, respectively:

$$\delta'_{\text{DCDM}} = -\theta_{\text{DCDM}} - m_{\text{cont}} - a\Gamma m_\psi \quad (7)$$

$$\theta'_{\text{DCDM}} = -\frac{a'}{a}\theta_{\text{DCDM}} + k^2 m_\psi \quad (8)$$

$$\delta'_\gamma = -\frac{4}{3}\theta_\gamma - \frac{4}{3}m_{\text{cont}} + a\Gamma \frac{\rho_{\text{DCDM}}}{\rho_\gamma} (\delta_{\text{DCDM}} - \delta_\gamma + m_\psi) \quad (9)$$

$$\theta'_\gamma = k^2 \left(\frac{1}{4}\delta_\gamma - \sigma_\gamma \right) + k^2 m_\psi + an_e \sigma_T (\theta_b - \theta_\gamma) - \frac{3}{4}a\Gamma \frac{\rho_{\text{DCDM}}}{\rho_\gamma} \left(\frac{4}{3}\theta_\gamma - \theta_{\text{DCDM}} \right) \quad (10)$$

$$F'_{\gamma,2} = 2\sigma'_\gamma = \frac{8}{15}\theta_\gamma - \frac{3k}{5}F_{\gamma,3} + \frac{8}{15}m_{\text{shear}} - \frac{9}{5}an_e \sigma_T \sigma_\gamma + \frac{1}{10}an_e \sigma_T (G_{\gamma,0} + G_{\gamma,2}) - 2\sigma_\gamma a\Gamma \frac{\rho_{\text{DCDM}}}{\rho_\gamma} \quad (11)$$

$$F'_{\gamma,\ell} = \frac{k}{2\ell+1} [\ell F_{\gamma,\ell-1} - (\ell+1)F_{\gamma,\ell+1}] - a\Gamma F_{\gamma,\ell} \frac{\rho_{\text{DCDM}}}{\rho_\gamma} \quad (12)$$

where the metric terms (m_{cont} , m_ψ , m_{shear}) depend on the gauge as written in Table II, σ_T is the Thomson cross-section, n_e is the electron density, G_γ is the difference between the two linear polarization components [105], and F_γ is the integrated perturbed phase-space distribution [106]:

$$F_\gamma = \frac{\int dq q^3 f_\gamma^0 \Psi_\gamma}{\int dq q^3 f_\gamma^0}, \quad (13)$$

with $F_{\gamma,\ell}$ the Legendre series expansion coefficients of this first-order quantity. In Eq. (13), q is the comoving photon spatial momentum and $f_\gamma^0 \equiv f_\gamma^0(q, \tau)$ is the unperturbed (background) part of the phase-space distribution, i.e., $f_\gamma(\vec{x}, \vec{q}, \tau) = f_\gamma^0(q, \tau)(1 + \Psi_\gamma(\vec{x}, \vec{q}, \tau))$, which defines the perturbation Ψ_γ . In the photon perturbation evolution equations, the new terms introduced in our model are those on the RHS of Eqs. (9)–(12) that are proportional to Γ ; the others are identical to those in the standard model [105]. The photon polarization evolution equations remain the same as in Λ CDM.

Gauge	Synchronous	Newtonian
m_{cont}	$h'/2$	$-3\phi'$
m_ψ	0	ψ
m_{shear}	$(h' + 6\eta')/2$	0

TABLE II: Metric terms appearing in the linear perturbation theory equations for our model, in the synchronous and Newtonian gauges ((h, η) and (ϕ, ψ) are the metric perturbations in these gauges; see Ref. [105] for definitions).

BBN Constraints

Due to the lower radiation density at early times, one might expect that BBN constraints could present a challenge to our scenario. Fortunately, the light element yields are predominantly controlled by $\hat{\omega}_b$, which is also the parameter combination involving ω_b and $T_{\text{CMB,ini}}$ to which the CMB is most sensitive [27]. Thus, our best-fit models yield BBN results that hardly differ from those of the best-fit Λ CDM model. We explicitly verify this result using the BBN code PRIMAT [103, 104]. For the best-fit DCDM γ (DCDM $\gamma + N_{\text{eff}}$) model to the full set of cosmological data, we find the He abundance $Y_{\text{P}} = 0.24720$ and D abundance $n_{\text{D}}/n_{\text{H}} = 2.444 \times 10^{-5}$ ($Y_{\text{P}} = 0.25074$ and $n_{\text{D}}/n_{\text{H}} = 2.480 \times 10^{-5}$), while for the best-fit Λ CDM model to *Planck* CMB data we have $Y_{\text{P}} = 0.24721$ and $n_{\text{D}}/n_{\text{H}} = 2.438 \times 10^{-5}$. Recent observational data yield $Y_{\text{P}} = 0.2449 \pm 0.0040$ [107] or $Y_{\text{P}} = 0.2446 \pm 0.0029$ [108], and $n_{\text{D}}/n_{\text{H}} = 2.527 \pm 0.030 \times 10^{-5}$ [109]. Our results are consistent with these measurements; in fact the DCDM γ and DCDM $\gamma + N_{\text{eff}}$ models improve the agreement with the D abundance data.

DCDM γ Results

A full compilation of the marginalized constraints on the DCDM γ model parameters is provided in Table III.

DCDM $\gamma + N_{\text{eff}}$ Analysis

Here we include results for the DCDM $\gamma + N_{\text{eff}}$ analysis (Table IV and Fig. 2), considering the same dataset combinations as used to constrain the DCDM γ model in the main text. The inclusion of DR (parameterized by N_{eff}) as an additional component in the model is motivated by (1) the fact that the DCDM component itself is likely to be (semi-)relativistic at recombination and (2) the need to mitigate the increase in Ω_{m} necessary to maintain the value of k_{eq} despite the lower photon energy density in the early universe (see discussion in the main text). Regarding point (1), strictly speaking the DCDM and DR components may in fact be identified with one another in the context of a specific particle physics model, i.e., it would be more correct to consider a “DR γ ” model

Constraints on Λ CDM γ Parameters

Parameter	<i>Planck</i> CMB TT+TE+EE, <i>FIRAS</i>	<i>Planck</i> CMB TT+TE+EE, <i>FIRAS</i> , SH0ES	<i>Planck</i> CMB TT+TE+EE, <i>FIRAS</i> , BAO, <i>Planck</i> $\phi\phi$, SNIa, RSD, DES-Y3	<i>Planck</i> CMB TT+TE+EE, <i>FIRAS</i> , BAO, <i>Planck</i> $\phi\phi$, SNIa, RSD, DES-Y3, Combined H_0
$T_{\text{CMB,ini}}$ [K]	2.710(2.718) $^{+0.016}_{-0.0024}$	2.617(2.587) $^{+0.044}_{-0.033}$	2.7158(2.7230) $^{+0.0093}_{-0.0023}$	2.712(2.709) $^{+0.013}_{-0.0044}$
$\log_{10}(\hat{\omega}_{\text{DCDM,ini}})$	$< -3.78(-4.35)$	$-3.77(-3.47)^{+0.66}_{-1.1}$	$< -3.82(-4.44)$	$< -3.74(-3.75)$
$\log_{10}(\frac{\Gamma}{\text{km/s/Mpc}})$	$> 3.36(5.01)$	$4.12(4.36)^{+0.89}_{-0.26}$	$> 3.75(5.67)$	$> 3.49(5.40)$
$\ln(10^{10} \hat{A}_s)$	$3.044(3.050) \pm 0.016$	$3.043(3.034) \pm 0.016$	$3.039(3.049) \pm 0.014$	$3.045(3.039) \pm 0.013$
n_s	$0.9647(0.9654) \pm 0.0043$	$0.9677(0.9677) \pm 0.0043$	$0.9671(0.9697) \pm 0.0037$	$0.9691(0.9679) \pm 0.0036$
$100\theta_s \times 10^4$	$10418.6(10418.1) \pm 3.0$	$10419.7(10421.0) \pm 3.0$	$10419.3(10420.1) \pm 2.8$	$10420.4(10419.3) \pm 2.8$
$\hat{\Omega}_b h^2 \times 100$	$2.234(2.237) \pm 0.015$	$2.242(2.230) \pm 0.015$	$2.243(2.250) \pm 0.013$	$2.252(2.237) \pm 0.014$
$\hat{\Omega}_c h^2$	$0.1201(0.1200) \pm 0.0014$	$0.1190(0.1192) \pm 0.0014$	$0.11878(0.11822) \pm 0.00092$	$0.11803(0.11859)^{+0.00083}_{-0.00099}$
τ_{reio}	$0.0541(0.0556) \pm 0.0076$	$0.0542(0.0481) \pm 0.0080$	$0.0531(0.0576) \pm 0.0069$	$0.0562(0.0536) \pm 0.0069$
δT_{CMB} [K]	$< 0.0535(0.0077)$	$0.109(0.138)^{+0.033}_{-0.044}$	$< 0.0279(0.0024)$	$< 0.0342(0.0169)$
H_0 [km/s/Mpc]	$67.82(67.59)^{+0.63}_{-0.88}$	$71.2(71.9) \pm 1.1$	$68.19(68.26) \pm 0.39$	$68.69(68.48) \pm 0.35$
$\Omega_c h^2$	$0.1180(0.1190)^{+0.0029}_{-0.0014}$	$0.1054(0.1020)^{+0.0047}_{-0.0040}$	$0.1175(0.1179)^{+0.0012}_{-0.00092}$	$0.1163(0.1164)^{+0.0013}_{-0.00095}$
Ω_m	$0.306(0.311)^{+0.015}_{-0.0090}$	$0.249(0.235) \pm 0.017$	$0.3019(0.3026)^{+0.0059}_{-0.0053}$	$0.2950(0.2963)^{+0.0056}_{-0.0050}$
σ_8	$0.8173(0.8164)^{+0.0085}_{-0.011}$	$0.850(0.860)^{+0.015}_{-0.020}$	$0.8089(0.8087)^{+0.0054}_{-0.0071}$	$0.8104(0.8120)^{+0.0064}_{-0.0078}$
S_8	$0.825(0.831)^{+0.019}_{-0.017}$	$0.774(0.761) \pm 0.018$	$0.8114(0.8122) \pm 0.0087$	$0.8035(0.8070) \pm 0.0081$
Age/Gyr	$13.823(13.809)^{+0.027}_{-0.041}$	$13.951(14.008)^{+0.062}_{-0.082}$	$13.796(13.773)^{+0.021}_{-0.029}$	$13.785(13.808)^{+0.024}_{-0.035}$
r_{drag} [Mpc]	$147.96(147.50)^{+0.31}_{-1.1}$	$153.3(155.1)^{+1.8}_{-2.5}$	$147.87(147.55)^{+0.26}_{-0.51}$	$148.1(148.3)^{+1.1}_{-0.87}$
$\chi^2_{\text{bf}, \text{Planck}}$	2764.3	2772.2	2764.8	2765.8
$\chi^2_{\text{bf}, \text{total}}$	2764.3	2773.2	3820.9	3838.0

TABLE III: Mean (best-fit) $\pm 1\sigma$ constraints on cosmological parameters in the Λ CDM γ model from various dataset combinations. Sampled parameters are shown in the first nine rows. Upper and lower limits are given at 95% CL. For comparison, a Λ CDM fit to *Planck* CMB + *FIRAS* yields $r_{\text{drag}} = 147.08(147.00) \pm 0.29$ Mpc and $\chi^2_{\text{bf}, \text{Planck}} = 2765.5$.

or a model with decaying warm dark matter, since the idea is that the decaying component is sufficiently light to contribute to N_{eff} at recombination. In the current implementation, we do not “remove” the additional N_{eff} energy density after recombination, i.e., it is simply taken to be a separate new species, in addition to the Λ CDM component. An explicit particle physics model may thus have fewer free parameters than considered here.

As for Λ CDM γ , primary CMB data alone do not show a strong preference for the Λ CDM γ + N_{eff} model over Λ CDM: we obtain $\Delta\chi^2 = -2.2$ in favor of Λ CDM γ + N_{eff} . The inclusion of SH0ES H_0 data yields a mild preference for non-zero Λ CDM, but less strong than in the (zero- N_{eff}) Λ CDM γ model, as here N_{eff} absorbs some of the change (although note that r_s^* is still increased here, relative to its Λ CDM value). Formally, the *Planck* CMB + *FIRAS* + SH0ES analysis yields an upper bound $\log_{10}(\hat{\omega}_{\text{DCDM,ini}}) < -3.15$ at 95% CL, with $H_0 = 71.3 \pm 1.2$ km/s/Mpc, $S_8 = 0.785^{+0.029}_{-0.022}$, and $\delta T_{\text{CMB}} < 0.193$ K, with a long tail extending to larger values than allowed in the analogous Λ CDM γ analysis (as anticipated by the inclusion of N_{eff}). The fit to *Planck* CMB data is only mildly degraded, with $\Delta\chi^2_{\text{Planck}} = 3.9$ compared to the best-fit Λ CDM model to *Planck* alone.

Removing SH0ES but including the full complement of non- H_0 datasets, the hint for Λ CDM weakens but is

notably stronger than for primary CMB data alone in the Λ CDM γ + N_{eff} analysis; here the DES-Y3 S_8 constraint plays an important role. However, the central value of H_0 does not increase compared to its primary-CMB value, despite the reduction in S_8 .

With all datasets combined (including all three independent H_0 probes), we find $H_0 = 69.88 \pm 0.79$ km/s/Mpc, $S_8 = 0.8088 \pm 0.0090$, and $\delta T_{\text{CMB}} < 0.0268$ K (95% CL upper limit). The Hubble constant is thus increased substantially more than in Λ CDM γ (where the analogous analysis yields $H_0 = 68.69 \pm 0.35$ km/s/Mpc), due to the role played by N_{eff} here. The error bar is also significantly increased, due to the parameter degeneracies in the radiation sector of this model. However, the fit to *Planck* is slightly degraded compared to that of Λ CDM, with $\Delta\chi^2_{\text{Planck}} = 3.5$; this very likely arises due to the *Planck* polarization data disfavoring large values of N_{eff} [31]. Note that the role played by the Λ CDM component here in increasing H_0 is now sub-dominant to the role played by N_{eff} via the standard sound-horizon reduction mechanism [25], as can be seen in the preferred values of r_{drag} , which now lie below the best-fit Λ CDM value.

For a final comparison, we fit a Λ CDM+ N_{eff} model to the full suite of datasets. Interestingly, we obtain H_0 values very similar to those found in the Λ CDM γ + N_{eff}

Constraints on $\Lambda\text{CDM}\gamma+N_{\text{eff}}$ Parameters

Parameter	<i>Planck</i> CMB TT+TE+EE, <i>FIRAS</i>	<i>Planck</i> CMB TT+TE+EE, <i>FIRAS</i> , SH0ES	<i>Planck</i> CMB TT+TE+EE, <i>FIRAS</i> , BAO, <i>Planck</i> $\phi\phi$, SNIa, RSD, DES-Y3	<i>Planck</i> CMB TT+TE+EE, <i>FIRAS</i> , BAO, <i>Planck</i> $\phi\phi$, SNIa, RSD, DES-Y3, Combined H_0
$T_{\text{CMB,ini}}$ [K]	$2.707(2.723)^{+0.019}_{-0.0020}$	$2.638(2.624)^{+0.068}_{-0.036}$	$2.711(2.713)^{+0.014}_{-0.0045}$	$2.7162(2.7182)^{+0.0091}_{-0.0021}$
$\log_{10}(\dot{\omega}_{\text{DCDM,ini}})$	$< -3.58(-4.44)$	$< -3.15(-3.36)$	$< -3.53(-4.04)$	$< -3.88(-4.29)$
$\log_{10}(\frac{\Gamma}{\text{km/s/Mpc}})$	$> 3.30(5.55)$	$4.07(4.76)^{+0.98}_{-0.50}$	$> 3.59(5.15)$	$> 3.74(5.13)$
$\ln(10^{10}\hat{A}_s)$	$3.036(3.039) \pm 0.018$	$3.051(3.054) \pm 0.019$	$3.028(3.036) \pm 0.016$	$3.051(3.052) \pm 0.014$
n_s	$0.9583(0.9572) \pm 0.0085$	$0.9722(0.9654)^{+0.0086}_{-0.0074}$	$0.9575(0.9626)^{+0.0081}_{-0.0072}$	$0.9763(0.9766) \pm 0.0055$
$100\theta_s \times 10^4$	$10422.6(10424.8) \pm 5.2$	$10417.2(10418.9) \pm 5.0$	$10425.5(10423.5) \pm 5.2$	$10415.4(10415.7) \pm 4.1$
$\hat{\Omega}_b h^2 \times 100$	$2.218(2.216) \pm 0.023$	$2.252(2.230)^{+0.024}_{-0.020}$	$2.219(2.234)^{+0.024}_{-0.020}$	$2.267(2.270) \pm 0.016$
$\hat{\Omega}_c h^2$	$0.1176(0.1161) \pm 0.0031$	$0.1207(0.1196) \pm 0.0031$	$0.1150(0.1162) \pm 0.0029$	$0.1214(0.1207) \pm 0.0023$
τ_{reio}	$0.0533(0.0556) \pm 0.0076$	$0.0560(0.0568)^{+0.0076}_{-0.0085}$	$0.0525(0.0549) \pm 0.0070$	$0.0556(0.0579) \pm 0.0072$
N_{ur}	$1.86(1.78) \pm 0.19$	$2.15(2.02)^{+0.20}_{-0.18}$	$1.77(1.86) \pm 0.18$	$2.25(2.22) \pm 0.13$
δT_{CMB} [K]	$< 0.0675(0.0028)$	$< 0.193(0.102)$	$< 0.0390(0.0126)$	$< 0.0268(0.0073)$
H_0 [km/s/Mpc]	$66.7(65.8) \pm 1.6$	$71.3(70.6) \pm 1.2$	$66.6(67.3) \pm 1.2$	$69.88(69.78) \pm 0.79$
$\Omega_c h^2$	$0.1152(0.1158)^{+0.0044}_{-0.0033}$	$0.1097(0.1068)^{+0.0097}_{-0.0069}$	$0.1131(0.1146) \pm 0.0034$	$0.1202(0.1197) \pm 0.0025$
Ω_m	$0.309(0.320)^{+0.018}_{-0.011}$	$0.258(0.256)^{+0.027}_{-0.020}$	$0.3054(0.3031) \pm 0.0066$	$0.2934(0.2934) \pm 0.0051$
σ_8	$0.811(0.804)^{+0.012}_{-0.016}$	$0.848(0.855)^{+0.017}_{-0.022}$	$0.8000(0.8043) \pm 0.0097$	$0.8178(0.8157) \pm 0.0082$
S_8	$0.823(0.829) \pm 0.018$	$0.785(0.789)^{+0.029}_{-0.022}$	$0.8071(0.8084) \pm 0.0094$	$0.8088(0.8067) \pm 0.0090$
Age/Gyr	$14.01(14.06) \pm 0.21$	$13.80(13.96)^{+0.21}_{-0.30}$	$14.08(13.97) \pm 0.20$	$13.57(13.59) \pm 0.13$
r_{drag} [Mpc]	$149.9(149.8)^{+2.0}_{-2.5}$	$151.0(152.9)^{+3.3}_{-5.4}$	$150.8(149.7)^{+2.0}_{-2.4}$	$145.8(146.0)^{+1.3}_{-1.5}$
N_{eff}	$2.87(2.79) \pm 0.19$	$3.17(3.04)^{+0.20}_{-0.18}$	$2.79(2.88) \pm 0.18$	$3.26(3.23) \pm 0.13$
$\chi^2_{\text{bf}, \text{Planck}}$	2763.3	2769.4	2764.3	2769.0
$\chi^2_{\text{bf}, \text{total}}$	2763.3	2773.5	3819.4	3834.3

TABLE IV: Mean (best-fit) $\pm 1\sigma$ constraints on cosmological parameters in the $\Lambda\text{CDM}\gamma+N_{\text{eff}}$ model from various dataset combinations. Sampled parameters are shown in the first ten rows. Upper and lower limits are given at 95% CL. The $\chi^2_{\text{bf}, \text{total}}$ for *Planck* CMB + *FIRAS* + SH0ES is slightly higher than that found in Table III because of small improvements in the fits to the *Planck* nuisance parameter priors, whose χ^2 contributions are not included here. For comparison, a ΛCDM fit to *Planck* CMB + *FIRAS* yields $r_{\text{drag}} = 147.08(147.00) \pm 0.29$ Mpc and $\chi^2_{\text{bf}, \text{Planck}} = 2765.5$, while a $\Lambda\text{CDM}+N_{\text{eff}}$ fit to the full combination of datasets considered in the rightmost column yields $H_0 = 70.04(70.28) \pm 0.78$ km/s/Mpc, $S_8 = 0.8101(0.8098) \pm 0.0090$, $r_{\text{drag}} = 144.9(144.6) \pm 1.2$ Mpc, $\chi^2_{\text{bf}, \text{Planck}} = 2771.5$, and $\chi^2_{\text{bf}, \text{total}} = 3834.8$.

fit, with $H_0 = 70.04 \pm 0.78$ km/s/Mpc, but the fit to the *Planck* CMB data is somewhat more degraded, with $\Delta\chi^2_{\text{Planck}} = 6.0$. The relative improvement of the *Planck* CMB fit in $\Lambda\text{CDM}\gamma+N_{\text{eff}}$ compared to $\Lambda\text{CDM}+N_{\text{eff}}$ is thus $\Delta\chi^2_{\text{Planck}} = -2.5$ in favor of the former. While this is not significant, it does indicate that the DCDM component helps in allowing the N_{eff} sound-horizon reduction mechanism to operate without degrading the fit to *Planck* as much as it otherwise would.

As in the $\Lambda\text{CDM}\gamma$ analysis, although the DCDM component is not detected, all dataset combinations disfavor low values of Γ (i.e., low z_X). In the *Planck*+*FIRAS*+SH0ES fit to $\Lambda\text{CDM}\gamma+N_{\text{eff}}$, the best-fit $z_X \simeq 75$; in the joint analysis of all datasets, the best-fit $z_X \simeq 130$ ($z_X \gtrsim 15$ at 95% CL). Thus, as found earlier, the (mildly) preferred decay redshifts are prior to reionization, where no direct observational constraints exist.

Our results indicate that small amounts of PRR are allowed, but tightly constrained, by background and linear cosmological observables. When additional DR is

included in the model, the bounds on PRR generally weaken slightly (although actually tighten slightly in the joint fit of all datasets), but still restrict the change in the CMB monopole temperature to $\lesssim 30\text{-}40$ mK and $f_{\text{DCDM}} \lesssim 0.2\text{-}0.3\%$. These bounds are completely independent from the spectral distortion signatures of such a scenario.

* Electronic address: jch2200@columbia.edu

† Electronic address: bb667@cam.ac.uk

- [1] G. Hinshaw, D. Larson, E. Komatsu, D. N. Spergel, C. L. Bennett, J. Dunkley et al., *Nine-year Wilkinson Microwave Anisotropy Probe (WMAP) Observations: Cosmological Parameter Results*, ApJS **208** (2013) 19 [1212.5226].
- [2] PLANCK collaboration, N. Aghanim et al., *Planck 2018 results. I. Overview and the cosmological legacy of Planck*, Astron. Astrophys. **641** (2020) A1 [1807.06205].
- [3] S. Aiola, E. Calabrese, L. Maurin, S. Naess, B. L.

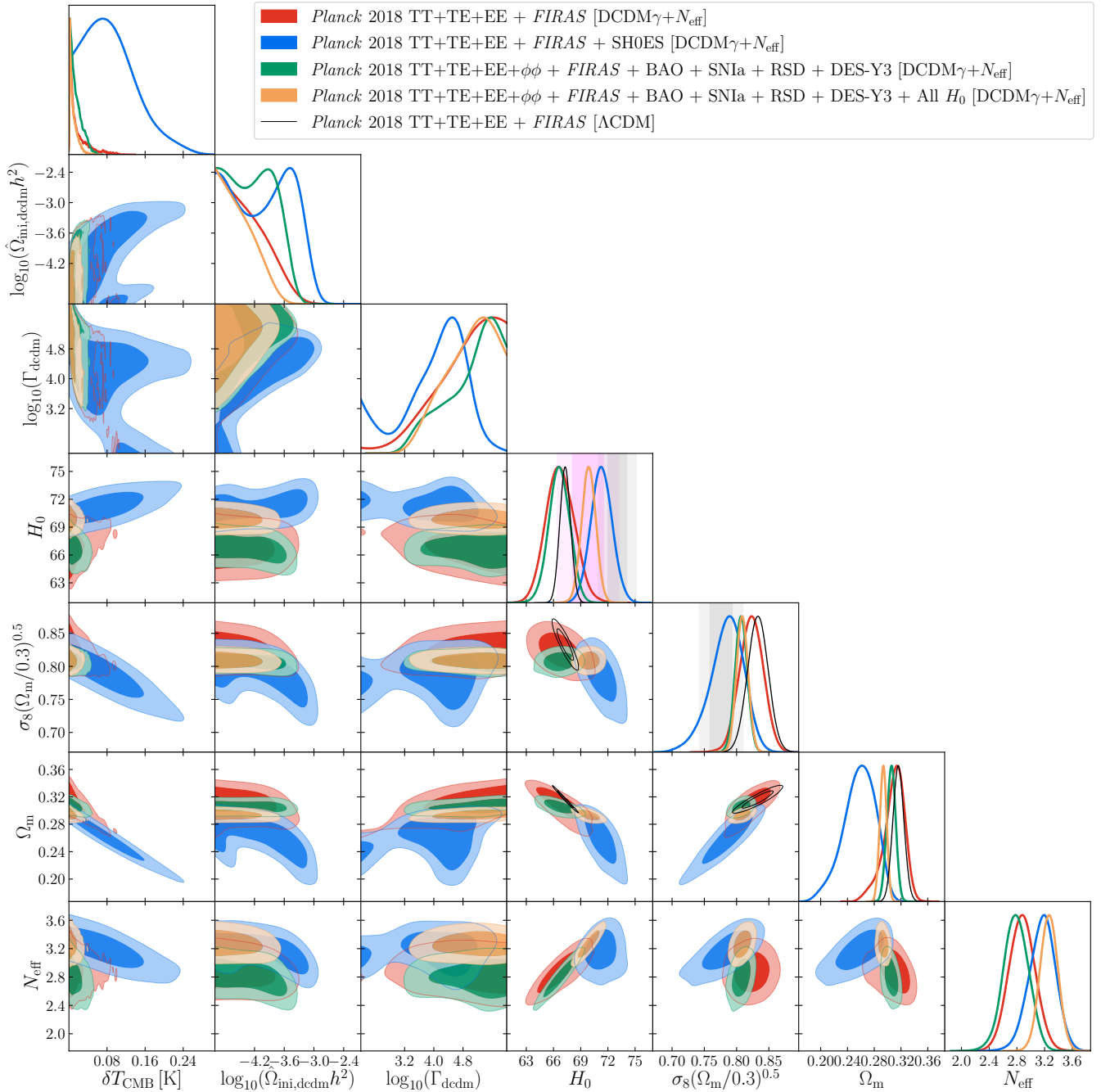


FIG. 2: Marginalized posteriors for the $\text{DCDM}\gamma+N_{\text{eff}}$ parameters and select other parameters in fits to various datasets, as labeled, with H_0 and Γ in units of km/s/Mpc.. For comparison, ΛCDM constraints for *Planck* CMB and *FIRAS* data are shown in thin black lines. The vertical grey and magenta bands are identical to those in Fig. 1.

- Schmitt, M. H. Abitbol et al., *The Atacama Cosmology Telescope: DR4 maps and cosmological parameters*, JCAP **2020** (2020) 047 [2007.07288].
- [4] SPT-3G collaboration, D. Dutcher et al., *Measurements of the E-mode polarization and temperature-E-mode correlation of the CMB from SPT-3G 2018 data*, Phys. Rev. D **104** (2021) 022003 [2101.01684].
- [5] A. G. Riess, S. Casertano, W. Yuan, L. M. Macri and D. Scolnic, *Large Magellanic Cloud Cepheid Standards Provide a 1% Foundation for the Determination of the Hubble Constant and Stronger Evidence for Physics beyond ΛCDM* , Astrophys. J. **876** (2019) 85 [1903.07603].
- [6] A. G. Riess, S. Casertano, W. Yuan, J. B. Bowers, L. Macri, J. C. Zinn et al., *Cosmic Distances Calibrated to 1% Precision with Gaia EDR3 Parallaxes and Hubble Space Telescope Photometry of 75 Milky*

- Way Cepheids Confirm Tension with Λ CDM, *Astrophys. J. Lett.* **908** (2021) L6 [2012.08534].
- [7] A. G. Riess et al., *A Comprehensive Measurement of the Local Value of the Hubble Constant with 1 km/s/Mpc Uncertainty from the Hubble Space Telescope and the SH0ES Team*, 2112.04510.
- [8] J. P. Blakeslee, J. B. Jensen, C.-P. Ma, P. A. Milne and J. E. Greene, *The Hubble Constant from Infrared Surface Brightness Fluctuation Distances*, *Astrophys. J.* **911** (2021) 65 [2101.02221].
- [9] DES collaboration, T. M. C. Abbott et al., *Dark Energy Survey Year 3 Results: Cosmological Constraints from Galaxy Clustering and Weak Lensing*, 2105.13549.
- [10] Planck Collaboration, P. A. R. Ade, N. Aghanim, M. Arnaud, M. Ashdown, J. Aumont et al., *Planck 2015 results. XXIV. Cosmology from Sunyaev-Zeldovich cluster counts*, *A&A* **594** (2016) A24 [1502.01597].
- [11] M. Asgari, C.-A. Lin, B. Joachimi, B. Giblin, C. Heymans, H. Hildebrandt et al., *KiDS-1000 cosmology: Cosmic shear constraints and comparison between two point statistics*, *Astronomy & Astrophysics* **645** (2021) A104.
- [12] A. Krolewski, S. Ferraro and M. White, *Cosmological constraints from unWISE and Planck CMB lensing tomography*, *JCAP* **12** (2021) 028 [2105.03421].
- [13] R. Dalal et al., *Hyper Suprime-Cam Year 3 Results: Cosmology from Cosmic Shear Power Spectra*, 2304.00701.
- [14] X. Li et al., *Hyper Suprime-Cam Year 3 Results: Cosmology from Cosmic Shear Two-point Correlation Functions*, 2304.00702.
- [15] DES collaboration, T. M. C. Abbott et al., *Dark Energy Survey Year 1 Results: A Precise H_0 Estimate from DES Y1, BAO, and D/H Data*, *Mon. Not. Roy. Astron. Soc.* **480** (2018) 3879 [1711.00403].
- [16] eBOSS collaboration, S. Alam et al., *Completed SDSS-IV extended Baryon Oscillation Spectroscopic Survey: Cosmological implications from two decades of spectroscopic surveys at the Apache Point Observatory*, *Phys. Rev. D* **103** (2021) 083533 [2007.08991].
- [17] O. H. E. Philcox, M. M. Ivanov, M. Simonović and M. Zaldarriaga, *Combining Full-Shape and BAO Analyses of Galaxy Power Spectra: A 1.6% CMB-independent constraint on H_0* , *JCAP* **05** (2020) 032 [2002.04035].
- [18] W. L. Freedman, B. F. Madore, T. Hoyt, I. S. Jang, R. Beaton, M. G. Lee et al., *Calibration of the Tip of the Red Giant Branch (TRGB)*, 2002.01550.
- [19] W. L. Freedman, *Measurements of the Hubble Constant: Tensions in Perspective*, *Astrophys. J.* **919** (2021) 16 [2106.15656].
- [20] S. S. Boruah, M. J. Hudson and G. Lavaux, *Peculiar velocities in the local Universe: comparison of different models and the implications for H_0 and dark matter*, *Mon. Not. Roy. Astron. Soc.* **507** (2021) 2697 [2010.01119].
- [21] S. Birrer et al., *TDCOSMO - IV. Hierarchical time-delay cosmography – joint inference of the Hubble constant and galaxy density profiles*, *Astron. Astrophys.* **643** (2020) A165 [2007.02941].
- [22] PLANCK collaboration, N. Aghanim et al., *Planck 2018 results. VIII. Gravitational lensing*, *Astron. Astrophys.* **641** (2020) A8 [1807.06210].
- [23] E. Di Valentino, O. Mena, S. Pan, L. Visinelli, W. Yang, A. Melchiorri et al., *In the realm of the Hubble tension—a review of solutions*, *Class. Quant. Grav.* **38** (2021) 153001 [2103.01183].
- [24] E. Abdalla et al., *Cosmology intertwined: A review of the particle physics, astrophysics, and cosmology associated with the cosmological tensions and anomalies*, *JHEAp* **34** (2022) 49 [2203.06142].
- [25] L. Knox and M. Millea, *Hubble constant hunter’s guide*, *Phys. Rev.* **D101** (2020) 043533 [1908.03663].
- [26] N. Schöneberg, G. Franco Abellán, A. Pérez Sánchez, S. J. Witte, V. Poulin and J. Lesgourgues, *The H_0 Olympics: A fair ranking of proposed models*, 2107.10291.
- [27] M. M. Ivanov, Y. Ali-Haïmoud and J. Lesgourgues, *H_0 tension or T_0 tension?*, *Phys. Rev. D* **102** (2020) 063515 [2005.10656].
- [28] D. J. Fixsen, *THE TEMPERATURE OF THE COSMIC MICROWAVE BACKGROUND*, *The Astrophysical Journal* **707** (2009) 916.
- [29] D. J. Fixsen, E. S. Cheng, J. M. Gales, J. C. Mather, R. A. Shafer and E. L. Wright, *The Cosmic Microwave Background Spectrum from the Full COBE FIRAS Data Set*, *ApJ* **473** (1996) 576 [astro-ph/9605054].
- [30] Y. Wen, D. Scott, R. Sullivan and J. P. Zibin, *Role of T_0 in CMB anisotropy measurements*, *Phys. Rev. D* **104** (2021) 043516 [2011.09616].
- [31] PLANCK collaboration, N. Aghanim et al., *Planck 2018 results. VI. Cosmological parameters*, *Astron. Astrophys.* **641** (2020) A6 [1807.06209].
- [32] SPT collaboration, A. Saro et al., *Constraints on the CMB Temperature Evolution using Multiband Measurements of the Sunyaev-Zel’dovich Effect with the South Pole Telescope*, *Mon. Not. Roy. Astron. Soc.* **440** (2014) 2610 [1312.2462].
- [33] G. Luzzi, R. T. Génova-Santos, C. J. A. P. Martins, M. De Petris and L. Lamagna, *Constraining the evolution of the CMB temperature with SZ measurements from Planck data*, *JCAP* **09** (2015) 011 [1502.07858].
- [34] A. Avgoustidis, R. T. Génova-Santos, G. Luzzi and C. J. A. P. Martins, *Subpercent constraints on the cosmological temperature evolution*, *Phys. Rev. D* **93** (2016) 043521 [1511.04335].
- [35] Y. Li, A. D. Hincks, S. Amodeo, E. S. Battistelli, J. R. Bond, E. Calabrese et al., *Constraining Cosmic Microwave Background Temperature Evolution With Sunyaev-Zel’dovich Galaxy Clusters from the Atacama Cosmology Telescope*, *ApJ* **922** (2021) 136 [2106.12467].
- [36] B. Bolliet, J. Chluba and R. Battye, *Spectral distortion constraints on photon injection from low-mass decaying particles*, *Monthly Notices of the Royal Astronomical Society* **507** (2021) 3148–3178.
- [37] C.-T. Chiang and A. Slosar, *Inferences of H_0 in presence of a non-standard recombination*, 1811.03624.
- [38] T. Sekiguchi and T. Takahashi, *Early recombination as a solution to the H_0 tension*, *Phys. Rev. D* **103** (2021) 083507 [2007.03381].
- [39] K. Jedamzik and L. Pogosian, *Relieving the Hubble tension with primordial magnetic fields*, *Phys. Rev. Lett.* **125** (2020) 181302 [2004.09487].
- [40] L. Thiele, Y. Guan, J. C. Hill, A. Kosowsky and D. N.

- Spergel, *Can small-scale baryon inhomogeneities resolve the Hubble tension? An investigation with ACT DR4*, *Phys. Rev. D* **104** (2021) 063535 [2105.03003].
- [41] B. Bolliet and J. C. Hill, *Resolving cosmic tensions with post-recombination reheating, to appear*.
- [42] A. Caputo, M. Regis, M. Taoso and S. J. Witte, *Detecting the Stimulated Decay of Axions at RadioFrequencies*, *JCAP* **03** (2019) 027 [1811.08436].
- [43] B. Audren, J. Lesgourgues, G. Mangano, P. D. Serpico and T. Tram, *Strongest model-independent bound on the lifetime of Dark Matter*, *JCAP* **2014** (2014) 028 [1407.2418].
- [44] S. Aoyama, T. Sekiguchi, K. Ichiki and N. Sugiyama, *Evolution of perturbations and cosmological constraints in decaying dark matter models with arbitrary decay mass products*, *JCAP* **2014** (2014) 021 [1402.2972].
- [45] D. Blas, J. Lesgourgues and T. Tram, *The Cosmic Linear Anisotropy Solving System (CLASS). Part II: Approximation schemes*, *JCAP* **2011** (2011) 034 [1104.2933].
- [46] F.-Y. Cyr-Racine, F. Ge and L. Knox, *Symmetry of Cosmological Observables, a Mirror World Dark Sector, and the Hubble Constant*, *Phys. Rev. Lett.* **128** (2022) 201301 [2107.13000].
- [47] VIRGO CONSORTIUM collaboration, R. E. Smith, J. A. Peacock, A. Jenkins, S. D. M. White, C. S. Frenk, F. R. Pearce et al., *Stable clustering, the halo model and nonlinear cosmological power spectra*, *Mon. Not. Roy. Astron. Soc.* **341** (2003) 1311 [astro-ph/0207664].
- [48] R. Takahashi, M. Sato, T. Nishimichi, A. Taruya and M. Oguri, *Revising the Halofit Model for the Nonlinear Matter Power Spectrum*, *ApJ* **761** (2012) 152 [1208.2701].
- [49] D. A. Riechers, A. Weiss, F. Walter, C. L. Carilli, P. Cox, R. Decarli et al., *Microwave background temperature at a redshift of 6.34 from H₂O absorption*, *Nature* **602** (2022) 58 [2202.00693].
- [50] F. Bianchini and G. Fabbian, *CMB spectral distortions revisited: A new take on μ distortions and primordial non-Gaussianities from FIRAS data*, *Phys. Rev. D* **106** (2022) 063527 [2206.02762].
- [51] J. Chluba, T. Kite and A. Ravenni, *Spectro-spatial evolution of the CMB I: discretisation of the thermalisation Green's function*, 2210.09327.
- [52] J. Chluba, A. Ravenni and T. Kite, *Spectro-spatial evolution of the CMB II: generalised Boltzmann hierarchy*, 2210.15308.
- [53] T. Kite, A. Ravenni and J. Chluba, *Spectro-spatial evolution of the CMB III: transfer functions, power spectra and Fisher forecasts*, 2212.02817.
- [54] J. Chluba, *Tests of the CMB temperature-redshift relation, CMB spectral distortions and why adiabatic photon production is hard*, *Mon. Not. Roy. Astron. Soc.* **443** (2014) 1881 [1405.1277].
- [55] Planck Collaboration, N. Aghanim, Y. Akrami, M. Ashdown, J. Aumont, C. Baccigalupi et al., *Planck 2018 results. V. CMB power spectra and likelihoods*, *A&A* **641** (2020) A5 [1907.12875].
- [56] A. J. Ross, L. Samushia, C. Howlett, W. J. Percival, A. Burden and M. Manera, *The clustering of the SDSS DR7 main Galaxy sample – I. A 4 per cent distance measure at $z = 0.15$* , *Mon. Not. Roy. Astron. Soc.* **449** (2015) 835 [1409.3242].
- [57] BOSS collaboration, S. Alam et al., *The clustering of galaxies in the completed SDSS-III Baryon Oscillation Spectroscopic Survey: cosmological analysis of the DR12 galaxy sample*, *Mon. Not. Roy. Astron. Soc.* **470** (2017) 2617 [1607.03155].
- [58] F. Beutler, C. Blake, M. Colless, D. H. Jones, L. Staveley-Smith, L. Campbell et al., *The 6dF Galaxy Survey: baryon acoustic oscillations and the local Hubble constant*, *MNRAS* **416** (2011) 3017 [1106.3366].
- [59] D. M. Scolnic et al., *The Complete Light-curve Sample of Spectroscopically Confirmed SNe Ia from Pan-STARRS1 and Cosmological Constraints from the Combined Pantheon Sample*, *Astrophys. J.* **859** (2018) 101 [1710.00845].
- [60] BOSS collaboration, S. Satpathy et al., *The clustering of galaxies in the completed SDSS-III Baryon Oscillation Spectroscopic Survey: On the measurement of growth rate using galaxy correlation functions*, *Mon. Not. Roy. Astron. Soc.* **469** (2017) 1369 [1607.03148].
- [61] J. C. Hill, E. McDonough, M. W. Toomey and S. Alexander, *Early dark energy does not restore cosmological concordance*, *Phys. Rev. D* **102** (2020) 043507 [2003.07355].
- [62] J. Torrado and A. Lewis, *Cobaya: Code for Bayesian Analysis of hierarchical physical models*, *JCAP* **05** (2021) 057 [2005.05290].
- [63] A. Gelman and D. B. Rubin, *Inference from Iterative Simulation Using Multiple Sequences*, *Statist. Sci.* **7** (1992) 457.
- [64] A. Gómez-Valent, *Fast test to assess the impact of marginalization in Monte Carlo analyses and its application to cosmology*, *Phys. Rev. D* **106** (2022) 063506 [2203.16285].
- [65] L. Hart and J. Chluba, *Updated fundamental constant constraints from Planck 2018 data and possible relations to the Hubble tension*, *Mon. Not. Roy. Astron. Soc.* **493** (2020) 3255 [1912.03986].
- [66] N. Lee, Y. Ali-Haïmoud, N. Schöneberg and V. Poulin, *What it takes to solve the Hubble tension through modifications of cosmological recombination*, 2212.04494.
- [67] S. K. Choi, M. Hasselfield, S.-P. P. Ho, B. Koopman, M. Lungu, M. H. Abitbol et al., *The Atacama Cosmology Telescope: a measurement of the Cosmic Microwave Background power spectra at 98 and 150 GHz*, *JCAP* **2020** (2020) 045 [2007.07289].
- [68] K. Surrao, B. Bolliet, J. C. Hill and O. Philcox, *Constraints on post-recombination reheating*, **in prep.**
- [69] X. Chen and M. Kamionkowski, *Particle decays during the cosmic dark ages*, *Phys. Rev. D* **70** (2004) 043502 [astro-ph/0310473].
- [70] L. Zhang, X. Chen, M. Kamionkowski, Z.-G. Si and Z. Zheng, *Constraints on radiative dark-matter decay from the cosmic microwave background*, *Phys. Rev. D* **76** (2007) 061301 [0704.2444].
- [71] J. T. Ruderman and T. Volansky, *Decaying into the hidden sector*, *Journal of High Energy Physics* **2010** (2010) 24 [0908.1570].
- [72] M. Ackermann, M. Ajello, A. Albert, B. Anderson, W. B. Atwood, L. Baldini et al., *Updated search for spectral lines from Galactic dark matter interactions with pass 8 data from the Fermi Large Area Telescope*, *Phys. Rev. D* **91** (2015) 122002 [1506.00013].

- [73] S. Ando and K. Ishiwata, *Constraints on decaying dark matter from the extragalactic gamma-ray background*, *JCAP* **2015** (2015) 024 [1502.02007].
- [74] N. Becker, D. C. Hooper, F. Kahlhoefer, J. Lesgourgues and N. Schöneberg, *Cosmological constraints on multi-interacting dark matter*, *JCAP* **02** (2021) 019 [2010.04074].
- [75] J. Jaeckel and W. Yin, *Shining ALP dark radiation*, *Phys. Rev. D* **105** (2022) 115003 [2110.03692].
- [76] K. Freese, F. C. Adams, J. A. Frieman and E. Mottola, *Cosmology with decaying vacuum energy*, *Nuclear Physics B* **287** (1987) 797.
- [77] J. M. Overduin, P. S. Wesson and S. Bowyer, *Constraints on Vacuum Decay from the Microwave Background*, *ApJ* **404** (1993) 1.
- [78] J. A. S. Lima, *Thermodynamics of decaying vacuum cosmologies*, *Phys. Rev. D* **54** (1996) 2571 [gr-qc/9605055].
- [79] R. Opher and A. Pelinson, *Decay of the vacuum energy into cosmic microwave background photons*, *MNRAS* **362** (2005) 167 [astro-ph/0409451].
- [80] A. C. Sobotka, A. L. Erickcek and T. L. Smith, *Was entropy conserved between BBN and recombination?*, *Phys. Rev. D* **107** (2023) 023525 [2207.14308].
- [81] N. Padmanabhan and D. P. Finkbeiner, *Detecting dark matter annihilation with CMB polarization: Signatures and experimental prospects*, *Phys. Rev. D* **72** (2005) 023508 [astro-ph/0503486].
- [82] S. Galli, F. Iocco, G. Bertone and A. Melchiorri, *CMB constraints on Dark Matter models with large annihilation cross-section*, *Phys. Rev. D* **80** (2009) 023505 [0905.0003].
- [83] M. S. Madhavacheril, N. Sehgal and T. R. Slatyer, *Current Dark Matter Annihilation Constraints from CMB and Low-Redshift Data*, *Phys. Rev. D* **89** (2014) 103508 [1310.3815].
- [84] T. R. Slatyer and C.-L. Wu, *General Constraints on Dark Matter Decay from the Cosmic Microwave Background*, *Phys. Rev. D* **95** (2017) 023010 [1610.06933].
- [85] D. Green, P. D. Meerburg and J. Meyers, *Aspects of Dark Matter Annihilation in Cosmology*, *JCAP* **04** (2019) 025 [1804.01055].
- [86] H. Liu, W. Qin, G. W. Ridgway and T. R. Slatyer, *Exotic energy injection in the early universe I: a novel treatment for low-energy electrons and photons*, **2303.07366**.
- [87] H. Liu, W. Qin, G. W. Ridgway and T. R. Slatyer, *Exotic energy injection in the early universe II: CMB spectral distortions and constraints on light dark matter*, **2303.07370**.
- [88] G. G. Raffelt, *Astrophysical axion bounds*, *Lect. Notes Phys.* **741** (2008) 51 [hep-ph/0611350].
- [89] J. Isern, E. García-Berro, S. Torres and S. Catalán, *Axions and the Cooling of White Dwarf Stars*, *ApJ* **682** (2008) L109 [0806.2807].
- [90] A. Ayala, I. Domínguez, M. Giannotti, A. Mirizzi and O. Straniero, *Revisiting the Bound on Axion-Photon Coupling from Globular Clusters*, *Phys. Rev. Lett.* **113** (2014) 191302 [1406.6053].
- [91] D. Tucker-Smith and N. Weiner, *Inelastic dark matter*, *Phys. Rev. D* **64** (2001) 043502 [hep-ph/0101138].
- [92] J. Alexander, M. Battaglieri, B. Echenard, R. Essig, M. Graham, E. Izaguirre et al., *Dark Sectors 2016 Workshop: Community Report*, p. arXiv:1608.08632, Aug., 2016, 1608.08632.
- [93] M. Baryakhtar, A. Berlin, H. Liu and N. Weiner, *Electromagnetic Signals of Inelastic Dark Matter Scattering*, *arXiv e-prints* (2020) arXiv:2006.13918 [2006.13918].
- [94] M. Carrillo González and N. Toro, *Cosmology and Signals of Light Pseudo-Dirac Dark Matter*, *arXiv e-prints* (2021) arXiv:2108.13422 [2108.13422].
- [95] A. Kogut, D. J. Fixsen, D. T. Chuss, J. Dotson, E. Dwek, M. Halpern et al., *The Primordial Inflation Explorer (PIXIE): a nulling polarimeter for cosmic microwave background observations*, *JCAP* **2011** (2011) 025 [1105.2044].
- [96] B. Maffei et al., *BISO: a balloon project to measure the CMB spectral distortions*, in *16th Marcel Grossmann Meeting on Recent Developments in Theoretical and Experimental General Relativity, Astrophysics and Relativistic Field Theories*, 10, 2021, 2111.00246.
- [97] J. Chluba et al., *Spectral Distortions of the CMB as a Probe of Inflation, Recombination, Structure Formation and Particle Physics: Astro2020 Science White Paper*, *Bull. Am. Astron. Soc.* **51** (2019) 184 [1903.04218].
- [98] J. Chluba et al., *New horizons in cosmology with spectral distortions of the cosmic microwave background*, *Exper. Astron.* **51** (2021) 1515 [1909.01593].
- [99] A. Kogut, M. H. Abitbol, J. Chluba, J. Delabrouille, D. Fixsen, J. C. Hill et al., *CMB Spectral Distortions: Status and Prospects*, **1907.13195**.
- [100] J. D. Hunter, *Matplotlib: A 2D Graphics Environment*, *Computing in Science and Engineering* **9** (2007) 90.
- [101] C. R. Harris, K. J. Millman, S. J. van der Walt, R. Gommers, P. Virtanen, D. Cournapeau et al., *Array programming with NumPy*, *Nature* **585** (2020) 357 [2006.10256].
- [102] A. Lewis, *GetDist: a Python package for analysing Monte Carlo samples*, **1910.13970**.
- [103] C. Pitrou, A. Coc, J.-P. Uzan and E. Vangioni, *Precision big bang nucleosynthesis with improved Helium-4 predictions*, *Phys. Rept.* **754** (2018) 1 [1801.08023].
- [104] C. Pitrou, A. Coc, J.-P. Uzan and E. Vangioni, *A new tension in the cosmological model from primordial deuterium?*, *Mon. Not. Roy. Astron. Soc.* **502** (2021) 2474 [2011.11320].
- [105] C.-P. Ma and E. Bertschinger, *Cosmological Perturbation Theory in the Synchronous and Conformal Newtonian Gauges*, *ApJ* **455** (1995) 7 [astro-ph/9506072].
- [106] M. Kaplinghat, R. E. Lopez, S. Dodelson and R. J. Scherrer, *Improved treatment of cosmic microwave background fluctuations induced by a late-decaying massive neutrino*, *Phys. Rev. D* **60** (1999) 123508 [astro-ph/9907388].
- [107] E. Aver, K. A. Olive and E. D. Skillman, *The effects of He I $\lambda 10830$ on helium abundance determinations*, *JCAP* **07** (2015) 011 [1503.08146].
- [108] A. Peimbert, M. Peimbert and V. Luridiana, *The primordial helium abundance and the number of neutrino families*, *Rev. Mex. Astron. Astrofis.* **52** (2016) 419 [1608.02062].

- [109] R. J. Cooke, M. Pettini and C. C. Steidel, *One Percent Determination of the Primordial Deuterium Abundance*, *Astrophys. J.* **855** (2018) 102 [1710.11129].